Vol 10 No 9, September 2001
1009-1963/2001/10(09)/0869-05

Chinese Physics

© 2001 Chin. Phys. Soc.
and IOP Publishing Ltd

REMARKABLE IMPROVEMENT OF THE COERCIVITY OF $TbMn_6Sn_6$ COMPOUND BY MELT-SPINNING PROCESS*

Zhao Peng(赵 鹏), Zhang Shao-ying(张绍英), Zhang Hong-wei(张宏伟),
Yan A-ru(阎阿儒), and Shen Bao-gen(沈保根)
State Key Laboratory of Magnetism, Institute of Physics and Centre for Condensed Matter Physics, Chinese Academy of Sciences, Beijing 100080, *China*

(Received 3 April 2001; revised manuscript received 9 May 2001)

The melt-spinning process has been carried out to improve the hard-magnetic properties of the $TbMn_6Sn_6$ compound. For the $TbMn_6Sn_6$ ribbons quenched at a rate of 40m/s and annealed at 545K for 30min, the highest coercivity of about 0.6T is achieved at room temperature, which is much higher than that of the $TbMn_6Sn_6$ ingot. Both the ingot and the ribbon coercivities will increase with decreasing temperature. For ribbons, a greater improvement of coercivity has been made at lower temperatures. Microstructural studies show the uniform nanocrystalline distribution in the $TbMn_6Sn_6$ ribbons and a small amount of Tb-rich phase in grain boundaries. The observed remarkable improvement of magnetic hardening in ribbons is believed to arise from the uniform nanoscale microstructure and the domain-wall pinning at the grain boundaries.

Keywords: melt-spinning process, nanoscale microstructure, coercivity
PACC: 7560G

I. INTRODUCTION

The series of RMn_6Sn_6 (R=rare-earth element) compounds with layered structures show a rich variety of magnetic properties because the Mn atoms carry a stable magnetic moment, and the competition between the intralayer and the interlayer exchange interactions gives rise to a sequence of magnetic structures when the temperature and the applied field strength are changed.[1] The magnetic structures and the magnetic properties of these compounds have been studied extensively, while the relatively low ordering temperature and low intrinsic coercive force at room temperature restrict their possible applications as permanent magnets. Among this class of compounds, $TbMn_6Sn_6$ crystallizes in the $HfFe_6Ge_6$-type structure (space group $P6/mmm$), which can be viewed as made of (001) planes containing alternately the magnetic Tb and Mn atoms, stacking along the c-axis with the sequence -Mn–Tb–Mn–Mn–Tb–Mn-. Throughout the range of the magnetic ordering temperature, the intralayer and interlayer Mn–Mn couplings are always ferromagnetic, while the interlayer Tb–Mn coupling is antiferromagnetic. This results in the collinear ferrimagnetic arrangement of this material. The $TbMn_6Sn_6$ compound also exhibits a reorientation of the easy magnetization direction from the c-axis to the ab-plane at 330K. At 2K, the magnetic moments of Tb and Mn are along the c-axis with $\mu(\mathrm{Mn}) = 2.4\mu_\mathrm{B}$ and $\mu(\mathrm{Tb})=8.6\mu_\mathrm{B}$, while at 300K, these magnetic moments are $\mu(\mathrm{Mn})=2.0\mu_\mathrm{B}$ and $\mu(\mathrm{Tb})=4.9\mu_\mathrm{B}$, and both deviate from the c-axis by an angle of 15°.[2] It has been reported that the $TbMn_6Sn_6$ compound presents a comparatively large coercivity of 1.12T at 4.2K, but at room temperature its coercivity is only about 0.03T.[3,4] Although some efforts have been made to develop the hard magnetic properties of the $TbMn_6Sn_6$ compound, the result was somewhat disappointing. For example, altering its composition not only lowered the magnetic ordering temperature of the $TbMn_6Sn_6$ compound, but also slightly lowered its hard magnetic properties.[5]

It is well known that melt-spinning and mechanical alloying are powerful techniques for developing suitable nanocrystalline microstructures in intermetallic compounds. Both methods have been successfully used to make various permanent magnets including Sm–Co, Nd–Fe–B, Sm–Fe–N(C) magnets.[6–8] In the past years, we have conducted extensive studies on nanostructured melt-spun 2:17-type carbides[9,10]

*Project supported by the State Key Project of Fundamental Research and the National Natural Science Foundation of China (Grant No. 19804017).

and Nd–Fe–B alloy.[11] In this paper, we will use melt-spinning to obtain the nanoscale microstructure and high coercivity in $TbMn_6Sn_6$ ribbons. The microstructure and the magnetic properties of this material will be reported and their relationship discussed.

Ⅱ. EXPERIMENT

The $TbMn_6Sn_6$ ingot was prepared by arc-melting the constituent materials Tb, Mn and Sn (with a purity of at least 99.9%) in highly purified argon gas. A 15% excess of Mn and a 5% excess of Tb were added to compensate for the loss of respective materials during the arc-melting process. The ingot was remelted at least three times to ensure homogeneity and annealed in an evacuated quartz tube at 1043K for 240h. The ribbons were made by melt-spinning the unannealed ingot onto a copper wheel in a highly pure argon atmosphere with the substrate velocity $\leq$40m/s. Then the ribbons were quenched at 40m/s and annealed at different temperatures for 30min in high vacuum. The crystal structure and the phases present were identified by X-ray diffraction (XRD) with Cu$K\alpha$ radiation. The microstructure was studied by optical microscopy and high resolution transmission electron microscopy (HRTEM) with energy dispersive X-ray (EDX) analysis for $TbMn_6Sn_6$ ingot and ribbons with optimum coercivity, respectively. Thermomagnetic curves for both the ingot and the ribbons were measured by a vibrating sample magnetometer (VSM) in a field of 0.05T. The hard magnetic properties were measured with a VSM under a maximum field of 1.9T at room temperature and with a superconducting quantum interference device (SQUID) magnetometer under a maximum field of 6T at different temperatures. Because the surface of the ribbons was vertical to the applied magnetic field when measured by SQUID, all the demagnetization curves for the $TbMn_6Sn_6$ ribbons were modified by the demagnetization factor N=1/3.

Ⅲ. RESULTS AND DISCUSSION

All the as-quenched $TbMn_6Sn_6$ ribbons obtained at $v \leq$40m/s were found to have hard magnetic behaviour. Our experimental results indicate that the coercivity of the ribbons quenched at 40m/s and annealed afterwards is higher than that of the ribbons straightly quenched at all the other cooling rates. Figure 1 shows the variation of coercivity at room temperature with annealing temperature (T_a), measured with a VSM in a field of 1.9T for $TbMn_6Sn_6$ ribbons quenched at 40m/s and subsequently annealed at temperatures from 480K to 733K for 30min in vacuum. It can be seen that after annealing at 545K for 30min, the coercivity of the $TbMn_6Sn_6$ ribbons can reach 0.6T at room temperature, much higher than that of $TbMn_6Sn_6$ reported previously.[4] We also notice that the coercivity at room temperature does not change much when the annealing time is longer than 30min. The XRD patterns show that these ribbons mainly consist of a $HfFe_6Ge_6$-type phase with a small amount of impurity phases appearing after melt-spinning. In addition, thermomagnetic curves also show that the Curie temperatures of the $TbMn_6Sn_6$ ingot and the ribbons are both about 423K. From Fig.1, the coercivity of the ribbons annealed at low temperatures is low, probably due to the existence of a more amorphous phase or due to the lack of enough crystallization of the hard magnetic 1:6:6 phase. However, the coercivity increases sharply with the increasing annealing temperature and reaches a maximal value of 0.6T at 545K. After that, the coercivity drops rapidly at higher annealing temperatures. This may be attributed to the increase in grain size and perhaps more impurities present in the ribbons.

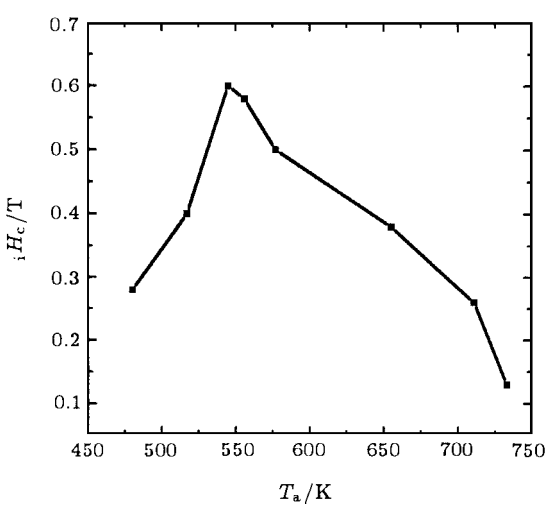


Fig.1. The variation of coercivity with annealing temperature (T_a) of the $TbMn_6Sn_6$ ribbons.

For the $TbMn_6Sn_6$ ingot and its ribbons annealed at 545K for 30min, the temperature dependence of coercivity ($_iH_c$) is shown in Fig.2. The high anisotropy field H_A of this material at low temperatures results in the high coercivity for both the ingot and the ribbons, as found in many rare-earth compounds previously.[12,13] For $TbMn_6Sn_6$ ribbons, we first measured the demagnetization curves at various temper-

atures without field-cooling. The coercivity increases up to about 2.5T at 150K and then decreases sharply with further decreasing temperature. However, the magnetization saturation below 150K is not reached and the demagnetization curves are very asymmetrical, indicating that the values of coercivity below 150K deviate from the realistic values of this material. Next, we measured the demagnetization curves of the ribbons while field-cooling; that is, applying a field of 6T at room temperature to saturate the material at first and then cooling down to the measuring temperature. The values of the coercivity below 150K are much higher than those measured without field-cooling. However, the material is still not magnetically saturated and the demagnetization curves are also asymmetrical, which can be seen in Figs.3 and 4. Thus, even by field-cooling, the values below 100K are still underestimated in our experiments. Moreover, the lower the measuring temperature, the more the results deviate. It is reasonable to deduce that the ribbons exhibit a continuous increase of H_c from 300K to 5K, and this is in agreement with the conclusion of the coercive field in the $TbMn_6Sn_6$ compound reported by Malaman *et al.*[4]

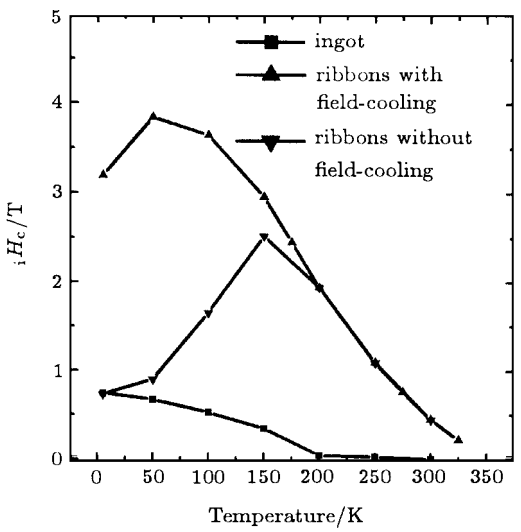


Fig.2. Temperature dependence of $_iH_c$ for the $TbMn_6Sn_6$ ingot and annealed ribbons.

Figure 3 shows the demagnetization curves for $TbMn_6Sn_6$ ribbons measured at various temperatures during field-cooling. At 300K, the coercivity of the ingot almost disappears while that of the ribbons still remains at about 0.5T, and the improvement of coercivity for this material can be further enhanced at lower temperatures.

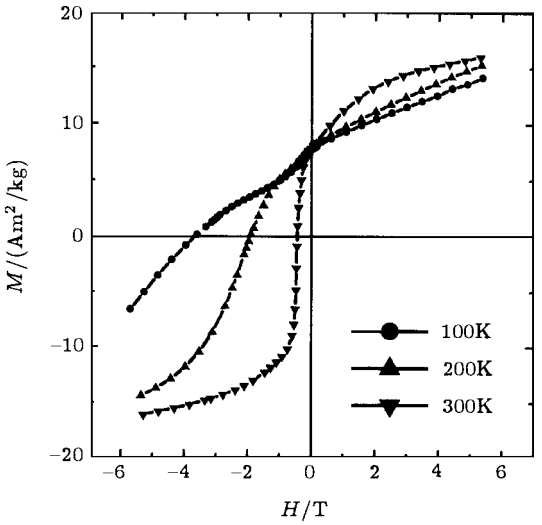


Fig.3. Typical demagnetization curves of the annealed $TbMn_6Sn_6$ ribbons at 100, 200 and 300K.

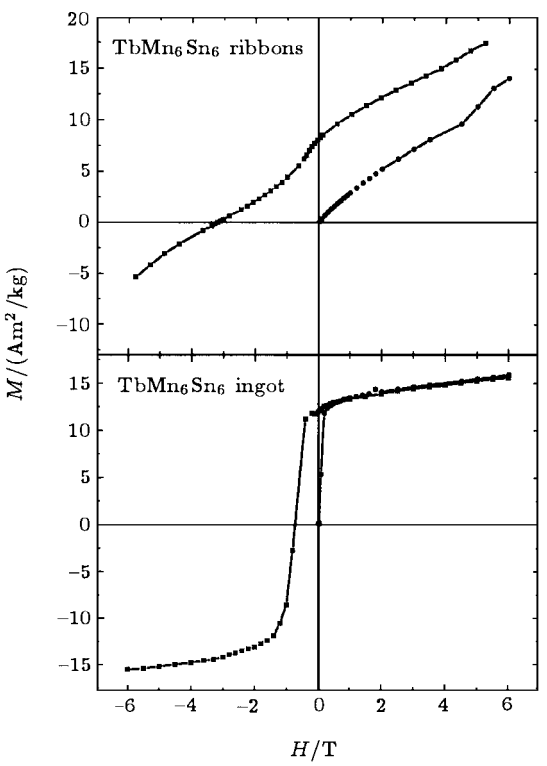


Fig.4. Initial magnetization and demagnetization curves for the $TbMn_6Sn_6$ ingot and annealed ribbons at 5K.

The initial magnetization behaviour of the $TbMn_6Sn_6$ ingot and ribbons at 5K, along with their demagnetization curves, are shown in Fig.4. For $TbMn_6Sn_6$ ribbons, the magnetization values under a field of 6T are different in the two curves because the demagnetization curve was measured at field-cooling. As discussed above, the demagnetization curve of the ribbons is very asymmetrical and the coercivity is even

lower than that at 50K. A knee can be observed in the demagnetization curve of $TbMn_6Sn_6$ ribbons in Fig.4, probably due to the presence of soft magnetic phases. For $TbMn_6Sn_6$ ribbons, the initial magnetization is marked by a low initial permeability, which then increases to a maximum when the field becomes comparable to its coercivity. This kind of magnetization is typical of domain-wall pinning at grain boundaries.[14] This result is in agreement with previously reported measurements on melt-spun $Sm_2(Fe,Ga)_{17}C_y$ and Nd–Fe–B ribbons.[15,16] Unlike the ribbons, the $TbMn_6Sn_6$ ingot shows a large initial permeability, indicating that the domain walls are initially free to move and can be swept through the sample under low fields. This is the typical coercivity mechanism of nucleation of reverse magnetization.



Fig.5. HRTEM image of the $TbMn_6Sn_6$ ribbons annealed at 545K for 30 min.

From the optical microscopy, we found that the typical grains of the $TbMn_6Sn_6$ ingot have an elongated shape. Most of the grains are about 80μm wide and about 800μm to 1200μm long. The HRTEM picture of $TbMn_6Sn_6$ ribbons annealed at 545K for 30min is shown in Fig.5. The typical grain size is about 20nm and most of the grains are also of an elongated shape resulting from the relatively low annealing temperature, unlike the equiaxed grains of previous 2:17-type ribbons, which were annealed at high temperatures.[10,17] The elongated grains vary in length from 20nm to 30nm, and hence the average grain size is distributed in a rather small range. EDX analysis reveals that most of the grains are of a 1:6:6-type phase, while there is a small amount of Tb-rich areas surrounding the 1:6:6-type grains. Both the uniform nanoscale grains and the phase rich in rare-earth element located in grain boundaries, greatly improve the hard magnetic properties of the $TbMn_6Sn_6$ ribbons.

As shown above, the remarkable improvement of coercivity of this material mainly comes from two essential differences between the $TbMn_6Sn_6$ ribbons and the ingot. On the one hand, the average grain size of the ingot is much larger than that of the ribbons.

As shown by HRTEM, the average grain size of the ribbons is smaller than the critical single domain particle size, thus the grains in the ribbons can be viewed as "single-domain particles". Because only magnetic moment rotation occurs in the magnetization and demagnetization processes in single-domain particles, the ribbons are difficult to magnetize and demagnetize so that they have low initial permeability and high coercivity. On the other hand, since the individual grains are smaller than the critical size, adjacent grains will interact with each other and well-defined domain walls will be formed by coalescence of domain walls from individual grains or group of grains. Consequently they are strongly pinned at the outer boundaries of these grains. In this case, the impurities of Tb-rich phases appearing at the grain boundaries in the ribbons provide the pinning sites. Therefore, the domain wall pinning at the grain boundaries also accomplishes the high coercivity of these ribbons. Similar conclusions have been made in the study of melt-spun Nd–Fe–B magnets.[18]

ACKNOWLEDGMENT

P Zhao would like to thank Professor Z H Cheng for valuable discussions.

References

[1] Venturini G, Chafik B, Idrissi El and Malaman B 1991 *J. Magn. Magn. Mater.* **94** 35

[2] Hu J F, Wang K Y, Hu B P, Wang Y Z, Wang Z X, Yang F M, Tang N, Zhao R W and Qin W D 1997 *J. Phys.: Condens. Matter* **7** 889

[3] Chafik B, Idrissi El, Venturini G and Malaman B 1991 *J. Less-Common Met.* **175** 143

[4] Malaman B, Venturini G, Welter R, Sanchez J P, Vulliet P and Ressouche E 1999 *J. Magn. Magn. Mater.* **202** 519

[5] Wang Y G, Yang F M, Chen C P, Tang N, Wang J L, Han X F, Pan H G, Hu J F, Zhou K W, Zhao R W and Wang Q D 1996 *J. Phys.: Condens. Matter* **8** 1851

[6] Hadjipanayis G C 1999 *J. Magn. Magn. Mater.* **200** 373

[7] Schultz L, Schnizke K, Wecker J, Katter M and Kuhrt C 1991 *J. Appl. Phys.* **70** 6339

[8] McCormick P G, Miao W F, Smith P A I, Ding J and Street R 1998 *J. Appl. Phys.* **83** 6256

[9] Zhang S Y, Sun Z G, Zhang H W, Han B S and Shen B G 1999 *Appl. Phys. Lett.* **75** 546

[10] Zhang H W, Sun Z G, Zhang S Y, Han B S and Shen B G 1999 *Phys. Rev.* B **60** 64

[11] Cheng Z H, Mao M X, Yang C L, Zhang Y D, Li F S, Shen B G, Zhang J X and Sun J J 1994 *Appl. Phys.* **76** 2981

[12] Zhang H W, Zhang S Y, Shen B G and Zhang L G 1997 *J. Phys. D: Appl. Phys.* **30** 3085

[13] Chen Z M, Meng-Burany X, Okumura H and Hadjipanayis G C 2000 *J. Appl. Phys.* **87** 3409

[14] Hilscher G, Grössinger R, Heisz S, Sassik H and Wiesinger G 1986 *J. Magn. Magn. Mater.* **54–57** 577

[15] Zhang S Y, Zhang H W, Shen B G, Zhan W S, Chin T S, de Boer F R and Buschow K H J 1999 *J. Appl. Phys.* **85** 2763

[16] Pinkerton F E and Van Wingerden D J 1986 *J. Appl. Phys.* **60** 3685

[17] Sun Z G, Zhang S Y, Zhang H W, Han B S and Shen B G 1999 *Acta Phys. Sin.* **48** S16 (in Chinese)

[18] Mishra R K 1986 *J. Magn. Magn. Mater.* **54–57** 450